Encapsulation and Coupling of Brownmillerite-Structured Active Oxides with Metallic Phase Change Materials for MultiModal Heat Storage and Air Separation

Yeku Wang[a], Shengxin Li[a], Ruijie Zhu[b], Nan Sheng[a], Chunyu Zhu[a]*

[a] School of Low-carbon Energy and Power Engineering, China University of Mining and Technology, Xuzhou, 221116, China

[b] Faculty of Engineering, Hokkaido University, N13-W8, Sapporo 060-8628, Japan

Corresponding Author:
Chunyu Zhu, E-mail: zcyls@cumt.edu.cn

Sample preparation

Table S1 presents the masses and dimensions of the as-prepared composite macrocapsules, thermochemical balls, and conventional phase change macrocapsules.

Table S1 Core/Shell Masses and Diameters

Samples	m_{core} (g)/D_{core}(mm)	m_{shell}(g)/D_{shell}(mm)	m_{total} (g)/D_{total}(mm)
Al-Si@CAMO	0.43/7	0.73/2	1.16/11
Al-Si@Al_2O_3@CAMO	0.29/6	Al_2O_3:0.92/1.5; CAMO:1.1/2	2.31/13
Al-Si@Al_2O_3	0.43/7	1.81/2	2.23/11
CAMO ball	-	1.12	1.12/11

Thermodynamic analysis of CAMO

Theoretically, the area of the thermal peak of the DSC curve should represent the enthalpy of the corresponding reaction. However, due to the inherent heat losses that occur during measurement, the enthalpy values obtained by the DSC thermal peaks are often less than the actual values. Instead, the chemical reaction enthalpy can be obtained by the famous Van't Hoff plot method based on obtaining the oxygen vacancy δ under different partial pressures.

The reduction reaction of CAMO is shown in Eq (1):

$$\frac{1}{\delta}\mathrm{Ca_2AlMnO_{5+\delta}} \leftrightarrow \frac{1}{\delta}\mathrm{Ca_2AlMnO_5} + \frac{1}{2}\mathrm{O_2} \tag{1}$$

Gibbs free energy is an important parameter describing the thermodynamic properties of chemical systems. By considering the change in Gibbs free energy for the reduction reaction in Eq (2), the key thermodynamics of the CAMO reduction process can be understood.

$$\Delta g_{\mathrm{O}} = \Delta h_{\mathrm{O}}^{\circ} - T\Delta s_{\mathrm{O}}^{\circ} + \frac{1}{2}RT\ln(\frac{P\mathrm{O_2}}{P^{\circ}}) \tag{2}$$

In the equation, the subscript O denotes per mole of oxygen atoms. This equation should equal zero at equilibrium, and rearranging it gives Eq (3):

$$\frac{P\mathrm{O_2}}{P^{\circ}} = A\exp(\frac{-2\Delta h_{\mathrm{O}}^{\circ}}{RT}),\quad A = \exp(\frac{2\Delta s_{\mathrm{O}}^{\circ}}{R}) \tag{3}$$

Through equation (3), it can be observed that the PO_2 exhibits an exponential dependence on the inverse of the reaction enthalpy and temperature. This implies that, at a constant temperature, a lower PO_2 can result in a greater enthalpy of reduction reaction.

Assuming that the sample volume was constant, the molar enthalpy and entropy for a given δ value could be calculated according to the Van't Hoff equation (4):

$$\frac{1}{2}\ln(\frac{PO_2}{P^o}) = \frac{-\Delta h_O^o}{RT} + \frac{\Delta s_O^o}{R}|_{\delta=\text{const}} \quad (4)$$

In this formula, PO_2 is the partial pressure of O_2, PO is the atmospheric pressure of 1 atm, and R is the ideal gas constant with a value of 8.314 J/ (K mol). By drawing the relationship between $\ln PO_2$ and 1/T, the molar enthalpy and molar entropy can be obtained, which are related to the slope of the linear fitted line and the Y-axis intercept respectively.

In this study, different oxygen partial pressures were obtained by controlling the amount of oxygen in the synthetic gas. Four fixed oxygen partial pressures of 1 atm, 0.5 atm, 0.2 atm and 0.1 atm were utilized to analyze the mass change of CAMO in the temperature range of 573K to 1073K. Under oxygen partial pressures of 1 atm and 0.2 atm, the TG curve of the CAMO sample is depicted in Figure S1.

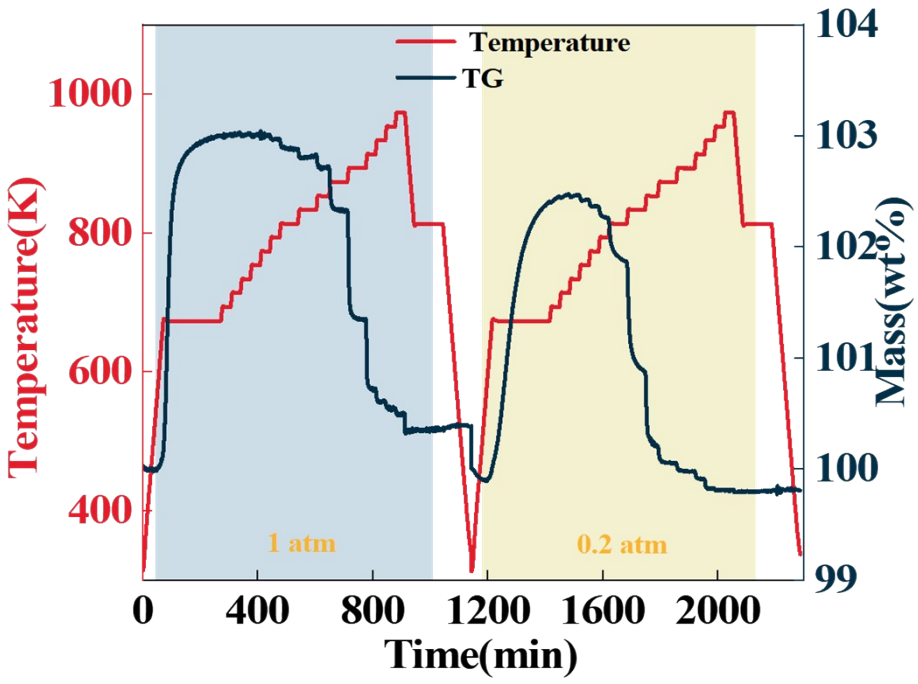

Figure S1 Schematic diagram of the CAMO test curves at 1 atm and 0.2 atm

Figure S1 depicts the δ values of the CAMO sample within a temperature range of 673 K to 1073 K under oxygen partial pressures of 1 atm and 0.2 atm. From Figure S1, it can be observed that δ decreases with increasing temperature and decreasing

oxygen partial pressure. This observation suggests that higher temperatures and lower oxygen partial pressures lead to the formation of more oxygen vacancies.

Table S2 presents the temperatures and oxygen partial pressures corresponding to various δ values.

Table S2 Temperature and oxygen partial pressure corresponding to different δ values

δ	Temperature(K)			
	0.1atm	0.2atm	0.5atm	1atm
0.05	578.46	605.33	633.93	658.96
0.1	565.42	588.21	616.98	646.18
0.15	556.03	577.65	611.75	639.81
0.2	549.24	571.38	606.49	633.44
0.25	542.46	565.11	600.63	626.82
0.3	529.23	557.47	594.63	618.65
0.35	509.46	543.82	585.48	607.58

Kinetic Analysis of CAMO

In the kinetic description of reaction (1), two distinct types of equations can be utilized to characterize the process:

$$\frac{d\alpha}{dt} = k(T)f(\alpha) \tag{5}$$

$$G(\alpha) = k(T)t \tag{6}$$

In the equation, $f(\alpha)$ and $G(\alpha)$ are the kinetic mechanism functions in differential and integral forms, respectively. α denotes the fraction of CAMO that has reacted at a given time, and is expressed as:

$$\alpha = \frac{\mathrm{m}_0 - m_t}{\mathrm{m}_0 - m_f} \tag{7}$$

It can be found that the relationship between $G(\alpha)$ and t should theoretically be linear. The reaction rate $k(T)$ can be evaluated by the slope, and the reaction model can be obtained through linear correlation. Since the reaction rate $k(T)$ is closely related to the temperature T, various scholars have proposed different forms of rate constant versus temperature, and the most used one is the Arrhenius equation, as shown in equation (8):

$$k(T) = A\exp(-\frac{E}{RT}) \tag{8}$$

where R is the gas constant. Integrating equation (8) yields equation (9), and it can be found that $\ln k(T)$ is linearly correlated with $1/T$, with its slope and intercept

corresponding to E and A, respectively.

$$\ln k(T) = \ln A - \frac{E}{RT} \tag{9}$$

For non-isothermal conditions:

$$T = T_0 + \beta t \tag{10}$$

In the equation (10), β represents the heating rate, (K/min).

Substituting equation (10) and equation (8) into equation (6) and then transforming, we obtain:

$$G(\alpha) = \int_0^{\alpha} \frac{d\alpha}{f(\alpha)} = \frac{A}{\beta}\int_0^{T} \exp(\frac{-E}{RT})dt = \frac{A}{\beta}\int_{T_0}^{T} \exp(\frac{-E}{RT})dt \tag{11}$$

Since equation (11) does not have an analytical solution for any temperature profile, it is necessary to introduce an approximate method. By substituting $u=E/(R\ T)$ into equation 11, we obtain:

$$G(\alpha) = \frac{A}{\beta}\int_0^{T} \exp(\frac{-E}{RT})dT = \frac{AE}{\beta R}\int_{\infty}^{u} \frac{-e^{-u}}{u^2}du = \frac{AE}{\beta R}P(u) \tag{12}$$

Introducing the Coats-Redfern approximation to calculate $P(u)$, and utilizing the Flynn-Wall-Ozawa (FWO) integral method to transform equation (12), we obtain:

$$\lg \beta = \lg\left(\frac{AE}{RG(\alpha)}\right) - 2.315 - 0.4567\frac{E}{RT} \tag{13}$$

The Malek method is used to ascertain the reaction mechanism $G(\alpha)$. This approach evaluates $G(\alpha)$ by comparing the degree of fit between experimental data and the predefined functions $y(\alpha)$ and $Z(\alpha)$. The functions $y(\alpha)$ and $Z(\alpha)$ are defined as follows:

$$y(\alpha) = (\frac{T}{T_{0.5}})^2 \frac{(\frac{d\alpha}{dt})}{(\frac{d\alpha}{dt})_{0.5}} = \frac{f(\alpha)G(\alpha)}{f(0.5)G(0.5)} \tag{14}$$

$$Z(\alpha) = \frac{\pi(u)(\frac{d\alpha}{dt})T}{\beta} = f(\alpha)G(\alpha) \tag{15}$$

In the equation (15), 0.5 represents the specific value when α=0.5, $\pi(u)$ is a rational number in the temperature integral equation with the expression $\pi(u)$ = 1/(u+2).

In isothermal reaction kinetics analysis, theoretical models are used for fitting as they provide a framework to explain the mechanism of chemical reactions and are relatively more reliable. The main steps in using this method are: firstly, a set of values for α and t are selected in the α-t curve at one temperature, with α=0.05 as one step increment in the study of this chapter. The obtained data are substituted into common $G(\alpha)$ models to linearly fit t. Theoretically, $G(\alpha)$ should be a straight line

with t, and the slope of the straight line is the reaction rate constant $k(T)$. Among these linear fits with t, the one with the best correlation should be the most reasonable reaction mechanism function. Then, using the same method, experimental data from several other temperatures are obtained, the mechanism function with the best linear correlation is fitted and processed, and a set of $k(T)$ values at different temperatures is derived. A linear fitting plot of $\ln k(T)$-$1/T$ is created, from which the remaining kinetic factors, namely the activation energy and the pre-exponential factor, are calculated based on the slope and intercept of the fitted line. Table S3 presents the mechanism function models for the kinetics of common chemical reactions. In the analysis of non-isothermal reaction kinetics, the FWO integral method is employed to directly determine the activation energy without selecting the reaction mechanism function, thus avoiding potential errors that may arise from different assumptions about the reaction mechanism. After the activation energy is determined, the Malek method is used to identify the most probable reaction mechanism function $G(\alpha)$. Finally, the pre-exponential factor is calculated after the reaction mechanism function has been determined.

Table S3 Common reaction kinetic models

Function name	Function type	f(α)	G(α)
F1/A1	First Order	$1-\alpha$	$-\ln(1-\alpha)$
F2	Quadratic Order	$(1-\alpha)^2$	$1/(1-\alpha)-1$
P2		$2\alpha^{1/2}$	$\alpha^{1/2}$
P3	Power Law	$3\alpha^{2/3}$	$\alpha^{1/3}$
P4		$4\alpha^{3/4}$	$\alpha^{1/4}$
R2	Geometric Contraction	$2(1-\alpha)^{1/2}$	$[1-(1-\alpha)^{1/2}]$
R3	Geometric Contraction (Ball)	$3(1-\alpha)^{2/3}$	$[1-(1-\alpha)^{1/3}]$
D1	One-dimensional Diffusion	$1/(2\alpha)$	α^2
D2	Two-dimensional Diffusion	$1/[-\ln(1-\alpha)]$	$(1-\alpha)\ln(1-\alpha)+\alpha$
D3	3-D Yonder Equation Ball	$[3(1-\alpha)^{2/3}]/[2-(1-\alpha)^{1/3}]$	$[1-(1-\alpha)^{1/3}]^2$
E1	Exponential law	α	$\ln\alpha$
A2		$2(1-\alpha)[-\ln(1-\alpha)]^{1/2}$	$[-\ln(1-\alpha)]^{1/2}$
A3	Avrami Erofeev	$3(1-\alpha)[-\ln(1-\alpha)]^{2/3}$	$[-\ln(1-\alpha)]^{1/3}$
A4		$4(1-\alpha)[-\ln(1-\alpha)]^{3/4}$	$[-\ln(1-\alpha)]^{1/4}$

The isothermal reduction reactions at 813K and 893K are shown in Figure S2. Upon atmosphere switching, CAMO undergoes rapid reduction followed by a plateau. The highest DTG of -1.23 wt%/min occurs at 893K, with total oxygen release of 2.3 wt%. Considering the gradual mass decrease with temperature, the total oxygen

release reaches approximately 2.8 wt%, indicating complete reaction. However, at 813K, despite forced reaction through atmosphere change, the total oxygen release is only about 2.6 wt%, demonstrating that CAMO is constrained by both temperature and oxygen partial pressure.

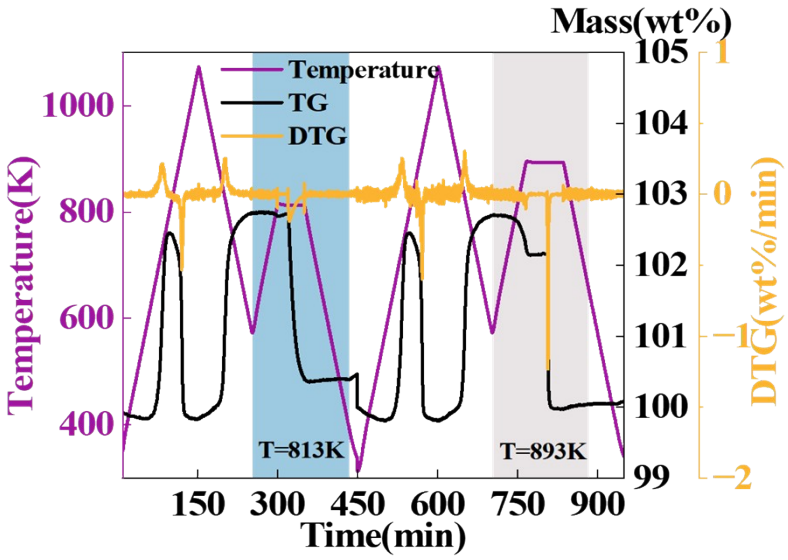

Figure S2 The isothermal reduction reactions at 813K and 893K

The conversion range of 0.1-0.8 during the fast reaction stage was selected for effective analysis (specific α-t data in Table S4). Temperature shows positive correlation with reaction efficiency, where increasing temperature significantly enhances conversion rate.

Table S4 Times for the conversion rate of reduction reaction to reach 0.1-0.8

α	Sample time (min)				
	813K	833K	853K	873K	893K
0.1	2.05	1.62	1.28	1.10	0.84
0.15	2.67	2.04	1.54	1.29	0.96
0.2	3.29	2.44	1.79	1.45	1.07
0.25	3.94	2.84	2.03	1.59	1.17
0.3	4.63	3.24	2.26	1.73	1.27
0.35	5.36	3.66	2.50	1.86	1.36
0.4	6.13	4.11	2.74	2.00	1.44
0.45	6.93	4.59	2.99	2.14	1.53
0.5	7.79	5.11	3.26	2.30	1.62
0.55	8.71	5.67	3.55	2.46	1.72
0.6	9.72	6.29	3.87	2.65	1.82
0.65	10.84	6.99	4.24	2.87	1.93
0.7	12.10	7.80	4.69	3.13	2.06
0.75	13.50	8.80	5.24	3.47	2.21
0.8	15.15	10.07	5.98	3.93	2.41

Based on the models shown in Table S3, by linearly fitting the kinetic functions, the R^2 for each function can be obtained, and the optimal fit is shown in Table S4.

Table S5 The results of fitting different models of CAMO reduction reaction at different temperatures

G(α)	Linear correlation coefficient at different temperatures R^2					
	1223K	1198K	1173K	1148K	1123K	average value
R3	**0.999**	**0.997**	**0.996**	**0.994**	**0.994**	**0.996**
F1	0.997	0.999	0.997	0.996	0.983	0.995

The isothermal oxidation reactions at 733K and 813K are shown in Figure S3. Upon atmosphere switching, CAMO undergoes rapid oxidation followed by slow progression. The DTG values at different temperatures are similar, approximately 0.43 wt%/min, with total oxygen uptake of 2.6 wt%. Including the gradual decrease with temperature reduction, the total oxygen release reaches about 2.8 wt%, indicating complete reaction.

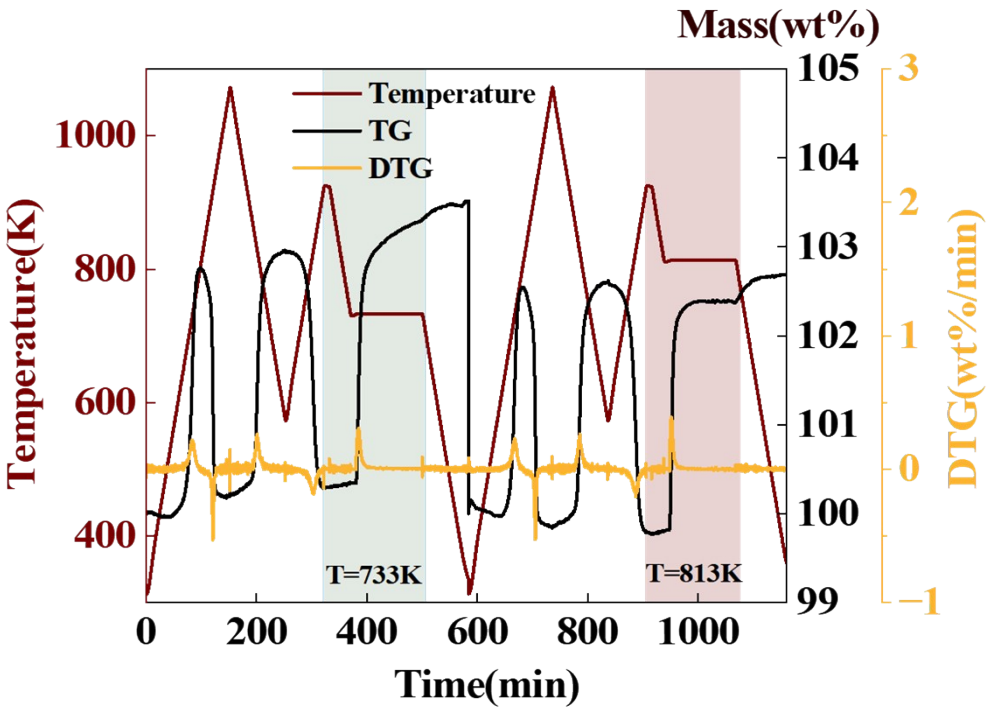

Figure S3 The isothermal reduction reactions at 733K and 813K

Although some crossover occurs between 813K and 793K at α=0.3, this doesn't affect the analysis, so the conversion range of 0.1-0.8 during the fast reaction stage remains selected as the effective analysis range (specific α-t data in Table S6).

Table S6 Times for the conversion rate of oxidation reaction to reach 0.1-0.8

α	Sample time (min)				
	733K	753K	773K	793K	813K
0.1	2.42	2.15	1.95	1.65	1.80
0.15	3.03	2.62	2.40	2.12	2.25
0.2	3.57	3.04	2.80	2.55	2.64
0.25	4.08	3.44	3.17	2.95	3.01
0.3	4.57	3.82	3.52	3.34	3.35
0.35	5.06	4.20	3.86	3.72	3.69
0.4	5.56	4.58	4.21	4.10	4.02
0.45	6.08	4.97	4.57	4.50	4.36
0.5	6.65	5.40	4.95	4.92	4.72
0.55	7.30	5.86	5.37	5.38	5.11
0.6	8.07	6.40	5.85	5.90	5.53
0.65	9.08	7.06	6.42	6.51	6.03
0.7	10.54	7.92	7.16	7.29	6.63
0.75	12.85	9.09	8.23	8.38	7.40
0.8	16.68	10.87	9.88	10.11	8.45

Based on the models shown in Table S3, by linearly fitting the kinetic functions, the R^2 for each function can be obtained, and the optimal fit is shown in Table S7.

Table S7 The results of fitting different models of CAMO oxidation reaction at different temperatures

G(α)	Linear correlation coefficient at different temperatures R^2					
	973K	1023K	1073K	1123K	1173K	average value
R3	0.940	0.981	0.981	0.985	0.995	0.977
D2	**0.971**	**0.985**	**0.982**	**0.982**	**0.974**	**0.979**

In the analysis of non-isothermal reaction kinetics, the FWO integral method is employed to directly determine the activation energy without selecting the reaction mechanism function, thus avoiding potential errors that may arise from different assumptions about the reaction mechanism. After the activation energy is determined, the Malek method is used to identify the most probable reaction mechanism function $G(\alpha)$. In the calculation of non-isothermal oxidation and reduction reactions, three of the four heating rates are processed based on the reliability of the data.

In the reduction reaction, the conversion curves at 10K and 15K nearly overlap in the range of 0.45-0.7. Therefore, considering data stability, the initial reaction stage (0.05-0.2), 0.25-0.4, and 0.75-0.95 were selected for analysis, with specific α-T values as shown in Table S8.

Table S8 Temperatures for the conversion rate of reduction reaction to reach 0.5-0.95

α	Temperature (K)				
	3K	5K	7K	10K	15K
0.05	811.62	821.33	840.03	849.89	854.21
0.1	855.35	863.02	872.26	880.44	882.86
0.15	882.71	886.56	890.86	893.86	894.33
0.2	894.62	897.69	899.57	901.50	901.61
0.25	901.37	903.35	904.66	906.11	906.12
0.3	905.20	907.13	907.98	909.34	909.37
0.35	907.98	909.94	910.52	911.81	911.95
0.4	910.10	912.11	912.71	914.15	914.16
0.75	920.23	922.83	923.72	925.62	926.90
0.80	921.70	924.47	925.44	927.48	929.17
0.85	923.49	926.34	927.47	929.77	931.93
0.90	925.86	928.89	930.14	932.85	935.54
0.95	930.21	933.80	934.91	938.65	942.72

Following the Flynn-Wall-Ozawa (FWO) integration method, the α-T data from Table S8 were substituted into Equation (S12) for fitting analysis, with the fitted curve shown in Figure S4.

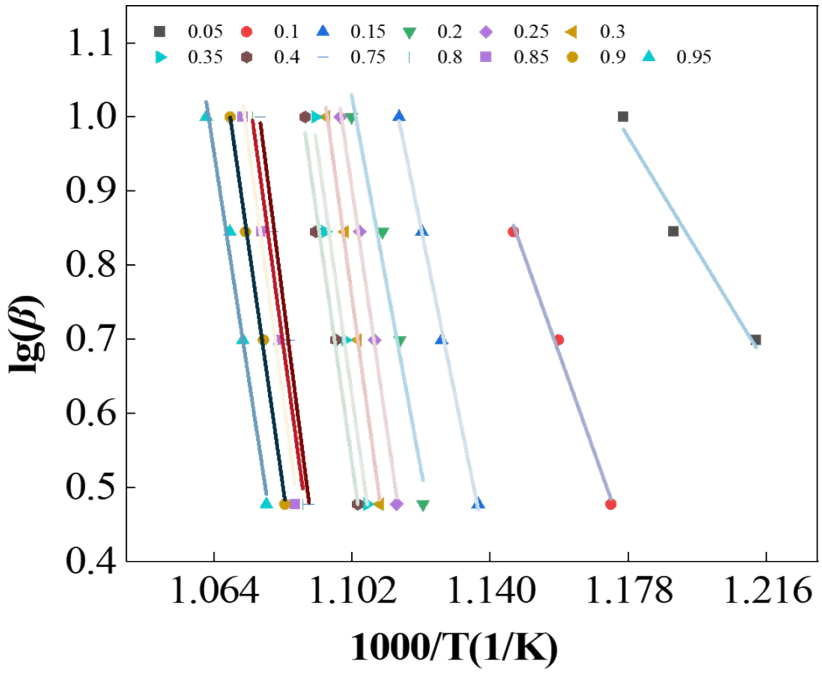

Figure S4 Linear fitting results for lg(β) and 1000/T in the reduction reaction of CAMO using the FWO integration method

The activation energies corresponding to different conversion rates can be obtained from the slopes of the fitted curves in Figure S4, and the calculated results are shown in Table S9.

Table S9 Activation energies corresponding to different conversion rates

α	E (kJ/mol)	R^2
0.05	164.06	0.986
0.1	250.87	0.997
0.15	439.27	0.998
0.2	482.99	0.973
0.25	614.54	0.996
0.3	652.85	0.995
0.35	636.10	0.986
0.4	629.78	0.988
0.75	697.48	0.996
0.80	656.91	0.982
0.85	652.51	0.985
0.90	624.69	0.998
0.95	582.73	0.989

The activation energies of the reduction range from 164.0669 to 697.4827 kJ/mol, with an average of 544.99 kJ/mol. The average activation energy in the initial stage is 334.30 kJ/mol, while the activation energy in the fast stage is relatively high at 645.61 kJ/mol.

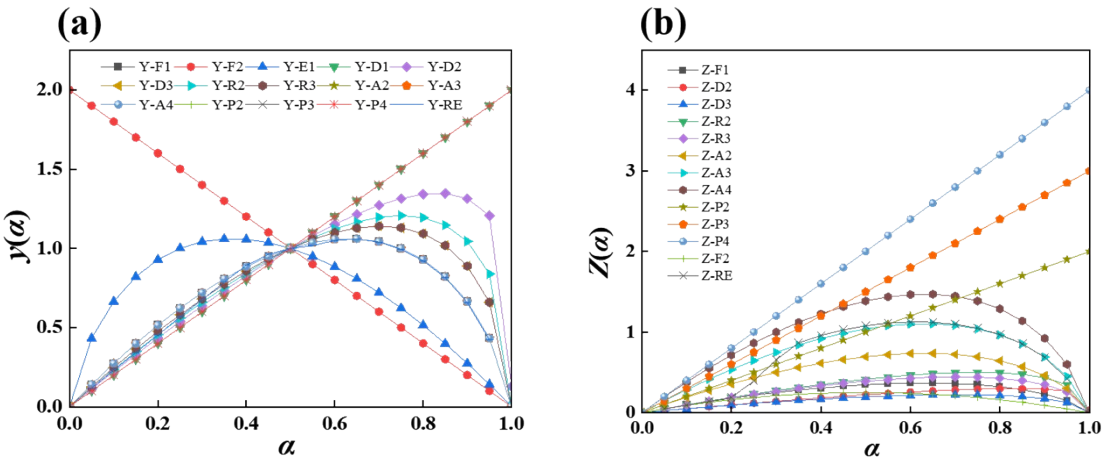

Figure S5 Comparison between experimental y(α) and Z(α) curves and theoretical models, (a)Comparison of $y(\alpha)$ curves calculated with experimental data curves, (b) Comparison of $Z(\alpha)$ curves calculated with experimental data curves.

The reaction mechanism function of the CAMO powder reduction process aligns with the shrinking core model (R3) and Avrami-Erofeev models (A3), with corresponding mechanism functions of $3(1-\alpha)^{2/3}$ and $3(1-\alpha)[-\ln(1-\alpha)]^{2/3}$. To further determine the activation energy of the fast reaction stage, the Phadnis method was employed to back-calculate the activation energy based on the known reaction mechanism. The formula is as follows:

$$G(\alpha)f(\alpha)=\frac{RT^2}{E}(\frac{d\alpha}{dt}) \tag{16}$$

This approach establishes that for an appropriate reaction mechanism, the term $G(\alpha)f(\alpha)$ exhibits a linear relationship with $T^2(d\alpha/dT)$, where the slope corresponds to R/E. Linear fitting for the latter reduction stage and initial oxidation stage, as depicted in Figure S6, yielded slopes of $1.39607\times10^{-5}$and 1.46897×10^{-5}, respectively. The corresponding activation energies were calculated to be 595.52 kJ/mol and 565.97 kJ/mol, respectively, with an average of 580.75kJ/mol. This value is slightly higher than the overall activation energy of the reduction reaction. The discrepancy primarily originates from alterations in the reaction mechanism and intrinsic errors associated with high-temperature measurements. In summary, the average activation energy is 334.30 kJ/mol for the initial stage of CAMO reduction, significantly higher at 580.75 kJ/mol for the fast stage, and 457.53 kJ/mol for the overall average activation energy.

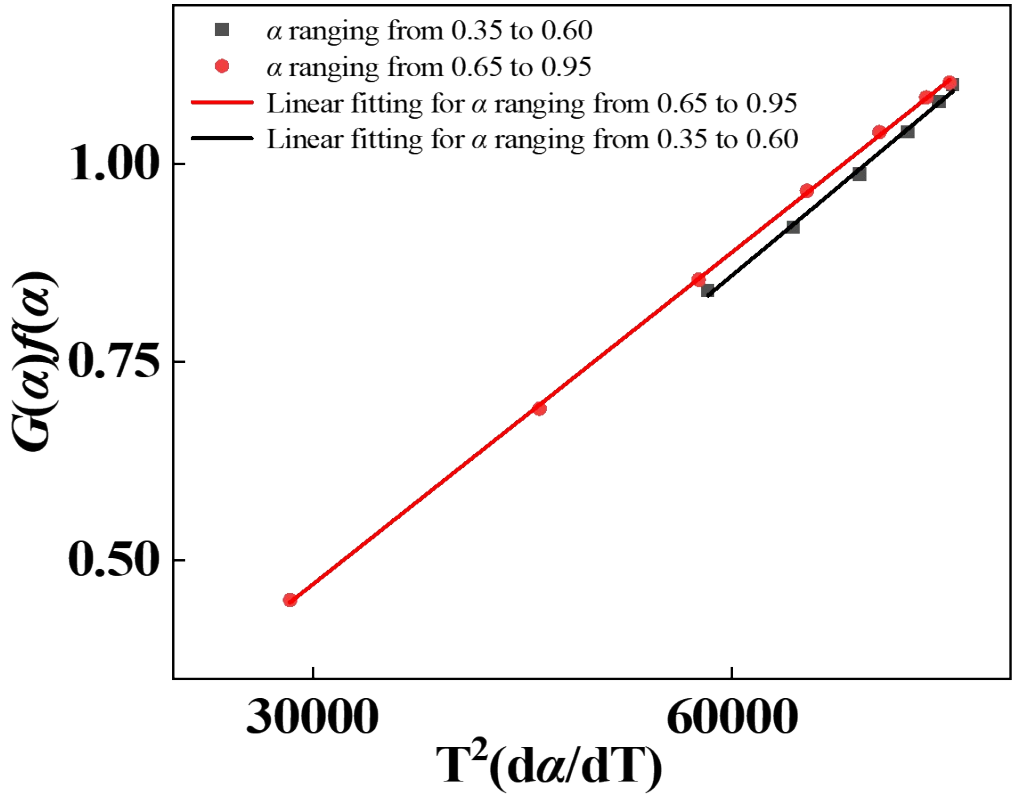

Figure S6 The linear relationship between G(α)f(α) and $T^2(d\alpha/dT)$ was evaluated using the Phadnis method

The oxidation conversion rates at heating rates of 3, 5, 7, 10, and 15 K/min are shown in Figure 4(e). The curves are consistent, with some overlap in the initial and final segments. The conversion range of 0.2-0.85 was selected for analysis, with specific α-T values in Table S10.

Table S10 Temperatures for the conversion rate of oxidation reaction to reach 0.2-0.85

α	Temperature (K)				
	3K	5K	7K	10K	15K
0.2	847.72	842.03	838.63	832.30	826.03
0.25	843.68	837.98	833.78	826.61	818.63
0.3	840.40	834.55	829.40	821.82	812.77
0.35	837.57	831.44	825.50	817.44	806.64
0.4	834.97	828.51	822.05	812.68	801.25
0.45	832.60	825.70	818.65	808.80	796.50
0.5	830.23	823.00	815.26	804.72	791.10
0.55	827.78	820.19	811.69	800.48	784.83
0.6	825.16	817.09	807.98	795.74	778.88
0.65	822.17	813.81	804.04	791.14	772.82
0.7	818.77	810.01	799.33	785.09	766.10
0.75	814.37	805.40	793.62	779.31	758.54
0.8	808.39	799.31	786.55	771.77	748.86
0.85	798.25	790.80	776.44	760.211	736.93

Using the Flynn-Wall-Ozawa (FWO) integration method, the α-T data from Table S10 were substituted into Equation (S13) for fitting analysis, and the fitted curve is presented in Figure S7.

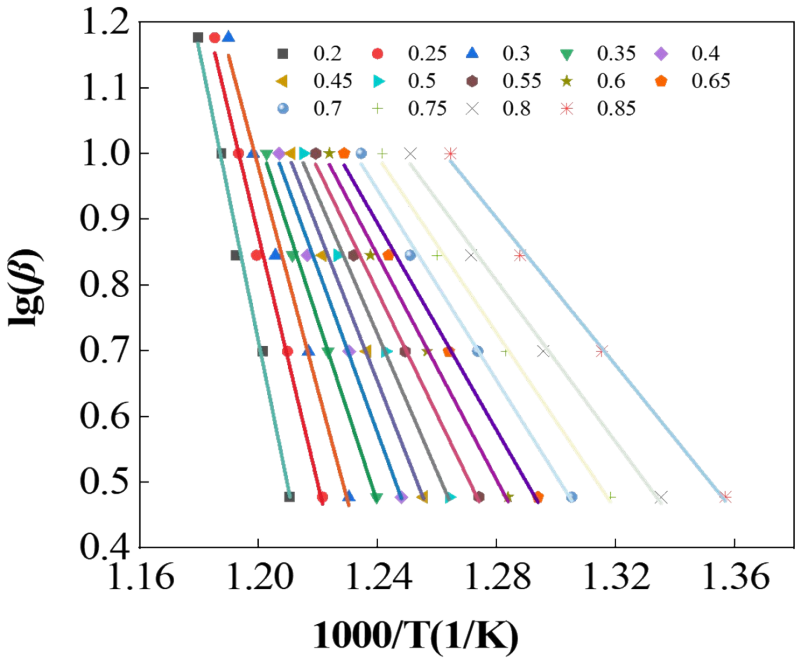

Figure S7 Linear fitting results for lg(β) and 1000/T in the oxidation reaction of CAMO using the FWO integration method

The activation energies corresponding to different conversion rates can be obtained by calculating the slopes of the fitted curves, and the calculated results are given in Table S11.

Table S11 Activation energies corresponding to different conversion rates

α	E (kJ/mol)	R^2
0.2	405.56	0.993
0.25	344.44	0.991
0.3	308.00	0.992
0.35	252.30	0.990
0.4	226.13	0.988
0.45	209.61	0.988
0.5	190.28	0.987
0.55	170.02	0.984
0.6	155.36	0.983
0.65	143.21	0.981
0.7	131.83	0.981
0.75	122.25	0.980
0.8	111.48	0.977
0.85	101.85	0.971

The corresponding reduction reaction process, when α is in the range of 0.2-0.85, has activation energies between 101.86 kJ/mol and 405.56 kJ/mol, with an average of 205.17 kJ/mol.

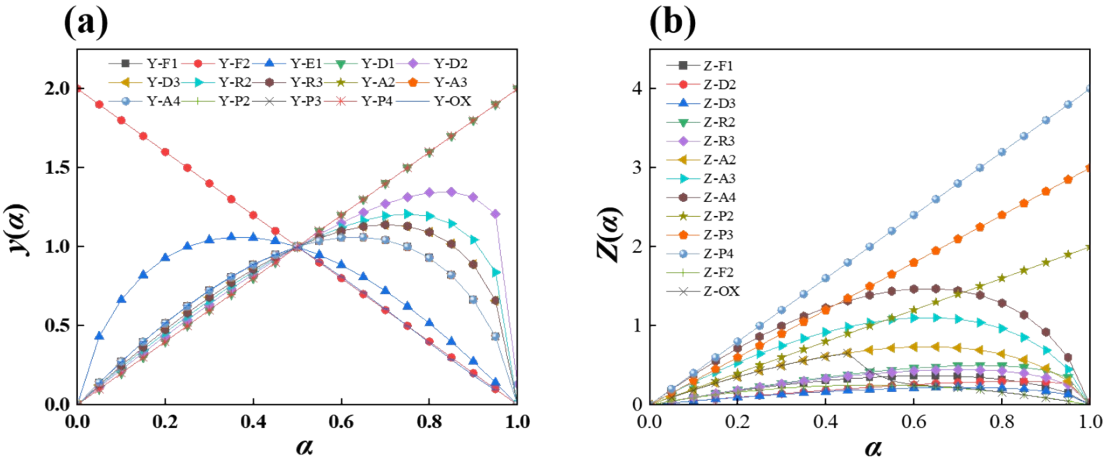

Figure S8 Comparison between experimental y(α) and Z(α) curves and theoretical models, (a)Comparison of $y(\alpha)$ curves calculated with experimental data curves, (b) Comparison of $Z(\alpha)$ curves calculated with experimental data curves.

Before α=0.45, the A2 model applies, transitioning to the F2 model after α=0.5 and 0.55. In the initial stage of the reaction, the surface of the oxygen-deficient CAMO reacts with oxygen, Oxygen molecules attack the most energetically favorable sites on the particle surface, forming oxidation product nuclei at these randomly distributed locations. These two-dimensional nuclei rapidly expand outward, begin to connect, and merge. As the reaction progresses, new nuclei continue to form and grow in uncovered areas, forming a thin, continuous oxidation product layer. Thereafter, the reaction can no longer proceed through two-dimensional surface expansion. The unreacted material is encapsulated beneath the product layer. The reaction front shifts from the external particle surface to the interface between the product layer and the unreacted core.